# Catalysis Science & Technology

Accepted Manuscript




This is an *Accepted Manuscript*, which has been through the Royal Society of Chemistry peer review process and has been accepted for publication.

*Accepted Manuscripts* are published online shortly after acceptance, before technical editing, formatting and proof reading. Using this free service, authors can make their results available to the community, in citable form, before we publish the edited article. We will replace this *Accepted Manuscript* with the edited and formatted *Advance Article* as soon as it is available.

You can find more information about *Accepted Manuscripts* in the Information for Authors.

Please note that technical editing may introduce minor changes to the text and/or graphics, which may alter content. The journal's standard Terms & Conditions and the Ethical guidelines still apply. In no event shall the Royal Society of Chemistry be held responsible for any errors or omissions in this *Accepted Manuscript* or any consequences arising from the use of any information it contains.



ROYAL SOCIETY OF CHEMISTRY

www.rsc.org/catalysis

Catalysis Science & Technology

Cite this: DOI: 10.1039/c0xx00000x

www.rsc.org/xxxxxx

PAPER

# Biodiesel Additive: Etherification of 5-Hydroxymethylfurfural with Isobutene into *tert*-Butoxymethylfurfural

**Feifei Yang[a], Shuguang Zhang[a], Z. Conrad Zhang[b], Jingbo Mao[a], Shenmin Li[a], Jingmei Yin[a], Jinxia Zhou*[a]**

***Received (in XXX, XXX) Xth XXXXXXXXX 20XX, Accepted Xth XXXXXXXXX 20XX***

***DOI: 10.1039/b000000x***

Biodiesel is a sustainable and environmentally compatible diesel fuel substitute that presents certain limitations, particularly low-temperature flow properties, which are attributable to its long fatty chain structure. Branched alkyl derivates such as tertiary butyl ethers are efficient biodiesel additives for improved cold flow behaviour in biodiesel. In this study, *tert*-butoxymethylfurfural (tBMF) is synthesised as a biodiesel additive through etherification of 5-hydroxymethylfurfural (5-HMF), a non-edible biomass-derived building block, with isobutene (IB) on a series of acid zeolites and liquid acids. The catalytic activity and selectivity of a zeolite catalyst involves not only optimisation of the number and strength of its acidic sites and adsorption properties but also promotion of its internal porespace. Efficient solvent systems did not include extremely weakly polar or strongly polar solvents but included moderately polar solvents, such as glycol dimethyl ether which presents suitable hydrophilic/hydrophobic properties. The HY zeolite with a $SiO_2/Al_2O_3$ mole ratio of 12 in combination with glycol dimethyl ether solvent exhibited an excellent tBMF selectivity of 94 mol% with 59 mol% 5-HMF conversion after 3 h of reaction at 60 ℃. Side reactions of 5-HMF dimerisation and the IB oligomerisation were minimal under mild reaction conditions. The activity of the deactivated catalyst was fully recovered by calcination in air, and a detailed deactivation mechanism was proposed.

## 1. Introduction

Diminishing fossil fuel reserves, growing concerns over global warming and environmental pollution have highlighted the need for utilisation of biomass resources as a renewable feedstock for production of fuels and chemicals.[1] Biodiesel, which is similar to typical petroleum-derived diesel composed of a mixture of $C_{11}$–$C_{22}$ compounds, has largely been produced through transesterification of triglycerides with methanol to form fatty acid methyl esters (FAME).[2] However, the long fatty chain structure of biodiesel yields poor low temperature properties (*i.e.*, high pour and cold filter plugging points), thereby resulting in cold flow issues (*e.g.*, high cloud point and viscosity) and unexpected emissions (*e.g.*, release of particles, hydrocarbons, carbon monoxide, *etc.*).[2] Isomerisation of long fatty chains into branched structures can improve the cold flow properties of biodiesel fuel, but such processes are generally achieved at higher temperatures and with low yields.[3] A low-energy intensive process for biodiesel reformulation involves the use of fuel additives.[2,4] Di-*tert*-butyl glycerol ethers and tri-*tert*-butyl glycerol ethers synthesised through etherification of glycerol with isobutene (IB) or *tert*-butanol have been used as biodiesel additives.[5] Addition of multi-*tert*-butyl glycerol ethers to biodiesel improves its low-temperature properties and reduces its viscosity.[6] Mono-*tert*-butyl glycerol ethers are unsuitable for use as diesel additives because their solubility in biodiesel is relatively low. Thus, one glycerol molecule must consume at least two molecules of the *tert*-butylation reagent for generation of valuable multi-butyl glycerol ethers. Moreover, glycerol has a

[a]*College of Environmental and Chemical Engineering, Dalian University, Dalian, China. Email: zhoujxmail@163.com; Tel: (+86)411-87403214; Fax: (+86)411-87402449*

[b]*Dalian National Laboratory of Clean Energy and State Key Laboratory of Catalysis, Dalian Institute of Chemical Physics, Chinese Academy of Sciences, Dalian, China.*

Catalysis Science & Technology Accepted Manuscript

low energy density because its C/O ratio is only 1.

5-Hydroxymethylfurfural (5-HMF) is an important non-edible biomass-derived building block that can be produced from glucose and fructose as well as polysaccharides such as cellulose and starch.[7,8] A 5-HMF molecule has only one hydroxyl group, and its C/O ratio is 2. Therefore, using 5-HMF as a basic feed for producing biodiesel additives not only saves the alkyl reagent but also yields high energy density and good combustion performance of the products.[4,9] Processes for producing 5-alkoxymethylfurfural mainly focus on the etherification of 5-HMF with $C_1$-$C_2$ alcohols in acid catalysis.[10-12] Branched and high-molecular weight alkyl derivatives, such as tertiary butyl ethers or tertiary butyl esters, are suitable for use as cold-flow improvers to reduce the viscosity of biodiesel because their structures present substantially better low-temperature flow properties .[6,13-15]

Both *tert*-butanol and IB are widely used to manufacture tertiary butyl ethers.[16] Today, however, few reports related to the preparation of *tert*-butoxymethylfurfural (tBMF) are available.[17,18] Gruter et al.[17] reported etherification of 5-HMF with *tert*-butanol; here, montmorillonite K10 and zeolite HY catalysed these reactions and resulted in 5-HMF conversions between 49% and 59% and tBMF selectivities between 76% and 79% at 100 ℃ under 12.5 bar of nitrogen. Salminen et al.[18] investigated the reaction in the toluene solvent catalysed by 1-butyl-3-methylimidazolium chloride ionic liquid ([BMIM]Cl) modified HBeta zeolites. The optimised result yielded a tBMF selectivity of 76%, which corresponds to a 5-HMF conversion of 46%. Etherification using IB achieves higher yields than that using *tert*-butanol during butyl glycerol ether synthesis.[16] In general, the use of IB is favoured because the excess reagent can be easily separated after the reaction from the liquid-phase products with a flash unit. However, to date, no experimental research on 5-HMF etherification with IB has yet been systematically reported.

The aim of the present study is to synthesis an attractive biodiesel additive, *i.e.*, tBMF, through etherification of 5-HMF with IB on acidic zeolites and homogeneous acids. Efforts are devoted to elucidate the mechanism of tBMF formation with the goal of understanding the roles of the catalyst and solvent and identifying critical factors determining product yield. Details of the relevant deactivation mechanism over the optimised catalyst under moderate operating conditions are elucidated, and catalyst regeneration via a simple method is explored.

## 2. Material and Methods

### 2.1. Materials

5-HMF (98%) was obtained from Aladdin (China). IB (99.5%) was purchased from Dalian Airchem Specialty Gases and Chemicals Co., Ltd. (China). Tetrahydrofuran (THF, 99%), dichloromethane (99%), *p*-toluenesulphonic acid (*p*-TSA, 99%) and acetonitrile (99%) were purchased from Sinopharm (China). Glycol dimethyl ether (99%) was supplied by Tianjin Guangfu Chemical Reagent Co., Ltd. (China). Diethylene glycol dimethyl ether (99%), toluene (99%), ethyl acetate (99%), dioxane (99%), concentrated sulphuric acid (97%) and cyclohexane (99%) were purchased from Tianjin Kermel Chemical Reagent Co., Ltd. (China). Acetone (99%) was purchased from Shenyang Xinxing Chemical Reagent Factory (China). Dimethylsulphoxide (99%) was supplied by Tianjin Damao Chemical Reagent Factory (China). Deionised water (DI $H_2O$) was supplied by Hangzhou Wahaha Group Co., Ltd. (China). All of the chemicals above were used as received.

The microporous zeolites used in the study, *i.e.*, $NH_4^+$Y (powder, $SiO_2/Al_2O_3$ mole ratio 5), $NH_4^+$Y (powder, $SiO_2/Al_2O_3$ mole ratio 12), HY (powder, $SiO_2/Al_2O_3$ mole ratio 80), $NH_4^+$Beta (powder, $SiO_2/Al_2O_3$ mole ratio 22), $NH_4^+$ZSM-5 (powder, $SiO_2/Al_2O_3$ mole ratio 80) and $NH_4^+$FER (powder, $SiO_2/Al_2O_3$ mole ratio 55), were supplied by Zeolyst International, Conshohocken, US. All zeolites were calcined at 550 ℃ to convert them into proton form and/or dehydrate residual moisture prior to their use. The zeolites were denoted as HY-5, HY-12, HY-80, HBeta-22, HZSM-5-80 and HFER-55. The numbers after the last dashed line correspond to the $SiO_2/Al_2O_3$ ratio in the zeolite structures. The properties of the zeolites used are shown in Table 1.

**Table 1.** Properties of the zeolites.

| Entry | Catalyst | $SiO_2/Al_2O_3$ mol/mol | $S_{BET}$ ($m^2$/g) | $V_{Pore}$ ($cm^3$/g) | Channel diameter (Å)[a] |
|---|---|---|---|---|---|
| 1 | HY-5 | 5 | 718 | 0.42 | [111]7.4&7.4 |
| 2 | HY-12 | 12 | 740 | 0.46 | [111]7.4&7.4 |
| 3 | HY-80 | 80 | 659 | 0.47 | [111]7.4&7.4 |
| 4 | HBeta-22 | 22 | 575 | 0.65 | [010]7.3&6.0[110]5.6&5.6 |
| 5 | HZSM-5-80 | 80 | 365 | 0.31 | [100]5.1&5.5[010]5.3&5.6 |
| 6 | HFER-55 | 55 | 361 | 0.24 | [001]4.2&5.4[010]3.5&4.8 |

[a] From Ref. 19.

### 2.2. Catalyst characterisations

X-ray powder diffraction (XRD) patterns were recorded at room temperature on a Rigaku Miniflex (M/s. Rigaku Corporation, Japan) X-ray diffractometer using Ni-filtered Cu Kα radiation (λ = 1.5406 Å) with a scan speed of 1 °/min and scan range of 2 °–80 ° at 30 kV and 15 mA. Scanning electron microscopy (SEM) images were obtained through a QUANTA 200FEG microscope. Thermogravimetric analysis (TGA) results were acquired using a TGA/SDTA851e instrument (Mettler Toledo). Samples were heated in a flow of $N_2$ gas (20 mL/min) from room temperature to 700 ℃ with a ramp rate of 10 ℃/min. Surface area measurement with nitrogen adsorption was performed with a Micromeritics ASAP 2020. The specific surface area ($S_{BET}$) was determined by the BET equation ($P/P^0$ = 0.05–0.3). The pore size distribution was determined from the desorption branch of the isotherm using Barrett–Joyner–Halenda theory. Temperature programmed desorption of ammonia ($NH_3$-TPD) was conducted on an AutoChem 2910 (Micromeritics) chemisorption system. Prior to analysis, all samples were subjected to calcination at 500 ℃ for 1 h in a helium flow of 20 mL/min. Then, the samples were cooled to 100 ℃ in He flow. Adsorption of 5% $NH_3$ in He was carried out at 100 ℃ for 1 h, followed by purging under a helium flow of 20 mL/min for 1 h at the same temperature. Desorption began from 100 ℃ with a temperature ramp of 10 ℃/min to 700 ℃. The amount of desorbed ammonia was quantified with a calibrated thermal conductivity detector. The natures of acid sites (Brønsted and Lewis) on the surfaces of zeolite catalysts were analyzed by Fourier transform infrared spectroscopy (FT-IR,

Catalysis Science & Technology Accepted Manuscript


This journal is © The Royal Society of Chemistry [year]

Bruker Equinox 55 FT-IR) with pyridine as a probe molecule. All catalyst samples were pretreated at 450 ℃ under vacuum for 2h to remove physically adsorbed water before pyridine adsorption at room temperature. Under vacuum, the pyridine saturated catalyst sample was heated at a rate of 10 ℃ /min to 150 ℃ for desorption. Spectra were taken after the sample was maintained at the desorption temperature for 20 min. Mass spectroscopy was performed on a GC–MS system (HP Agilent 6890N-5973N). Proton nuclear magnetic resonance (1H NMR) spectra were recorded using a Bruker AVANCE AV-500 NMR spectrometer at a frequency of 300 MHz ($CDCl_3$, TMS as internal standard).

### 2.3. Catalytic performance measurement

Etherification experiments were performed in oil-bath-heated stainless steel autoclaves (15 mL) equipped with feedstock line connectors and pressure gauges. Temperatures and stirring rates were controlled by IKA magnetic Stirrers (IKA-Werke GmbH & Co. KG, Germany). The stirring rate was set at 1000 rpm to overcome external diffusion limitations. The feed mixture was composed of 100 mg of 5-HMF in 1 mL solvent, IB:5-HMF mole ratio ($R_{IB/5\text{-}HMF}$) varying from 2:1 to 6:1 and catalyst loadings (wt% with respect to the 5-HMF mass) varying from 5 wt% to 50 wt%. In a typical run, a specific amount of 5-HMF, dry catalyst and solvent were loaded into the autoclave and sealed. After the autoclave was flushed with nitrogen to remove air, IB was injected into the reactor. The liquid isobutene was first charged into a sample loop which has a specified volume. Then the isobutene in the sample loop was injected into the reactor under nitrogen pressure. The initial pressure in the autoclave was adjusted to 1.0 MPa with nitrogen. The oil bath was preheated to a given temperature, and counting of the reaction time began as soon as the autoclave was placed in the bath. Each reaction usually lasted for 3 h at a specific temperature. After a specified reaction period, the reaction was quenched immediately with cool water. Unreacted IB was collected using a rubber gas bag by repeated releasing and flushing of the reactor with $N_2$. The gas composition in the rubber gas bag was analysed by GC. The liquid mixture obtained after the reaction was mixed with a given amount of diethylene glycol dimethyl ether as an inert internal standard, diluted with glycol dimethyl ether and then filtered to remove the catalyst for compositional analysis by GC. The used catalyst recovered from the reaction mixture by filtration was washed thrice with dichloromethane and ethyl acetate and then dried overnight at 80 ℃ in a vacuum oven. The recovered catalyst was used as "spent HY-12" in a second reaction cycle under the same reaction conditions. The catalyst recovered from the second reaction cycle was then washed, calcined in air at 550 ℃ for 3 h and used as "calcined HY-12" for a third cycle.

GC analysis was conducted on a GC (HP5890) equipped with a flame ionisation detector. The column used was a PEG2W capillary column (30 m × 0.32 mm × 0.5 μm) manufactured by Dalian Institute of Chemical Physics, Chinese Academy of Sciences. Commercial compounds of 5-HMF, IB, 2,4,4-trimethyl-1-pentene (98%, Aldrich, representative of di-isobutylene [DiB]) and homemade 5,5'-(oxy-bis(methylene))bis-2-furfural (OBMF) were used as standard references to determine the corresponding response factors. OBMF (98%) was synthesised, purified according to the methods described by Casanova et al.[20] and confirmed by $^1$H NMR and GC-MS spectrometry. Results reported for 5-HMF conversion, tBMF selectivity and tBMF and OBMF yields are expressed in mol% based on the total molar amount of 5-HMF intake. The extent of IB oligomerisation (DiB wt%) was calculated in terms of mass percentages of DiB with respect to the total IB originally loaded in the reactor.

## 3. Results and Discussion

### 3.1. Catalyst selection and reaction pathways

**Table 2.** Catalytic performance of the acid catalysts for 5-HMF etherification with IB[a]

| Entry | Catalyst | Conversion (mol%) | Selectivity (mol%) | Yield (mol%) | | DiB (wt%) |
|---|---|---|---|---|---|---|
| | | 5-HMF | tBMF | tBMF | OBMF | |
| 1 | HY-5 | 5 | - | - | - | - |
| 2 | HY-12 | 59 | 94 | 55 | <1 | <1 |
| 3 | HY-80 | 45 | 95 | 43 | <1 | <1 |
| 4 | HBeta-22 | 24 | 71 | 17 | 2 | 3 |
| 5 | HZSM-5-80 | 5 | - | - | - | - |
| 6 | HFER-55 | 2 | - | - | - | - |
| 7 | *p*-TSA | 43 | 10 | 4 | 23 | <1 |
| 8 | $H_2SO_4$ | 62 | 27 | 17 | 8 | <1 |

[a] Reaction conditions: $R_{IB/5\text{-}HMF}$, 4 mol/mol; catalyst loading of entries 1-6 = 30 wt% with respect to 5-HMF mass; catalyst loading of entries 7 and 8 = 5 wt% with respect to 5-HMF; 100 mg 5-HMF in 1 mL of glycol dimethyl ether solvent; 60 ℃; 3 h.

A series of zeolite solid acid catalysts and two types of liquid acids, *i.e.*, *p*-TSA and $H_2SO_4$, were used to catalyse 5-HMF etherification with IB at 60 ℃. The catalytic performances of the catalysts are shown in Table 2. Etherification of 5-HMF with IB by Brønsted acid occurs through an electrophilic substitution reaction catalysed by acids (Scheme 1). The initial step of this reaction involves protonation of IB to form a *tert*-butyl cation (t-$C_4H_9^+$), followed by electrophilic reaction of t-$C_4H_9^+$ with the O of the hydroxyl group of 5-HMF to form an intermediate. Finally, the desired product, tBMF, is formed through removal of $H^+$ from the intermediate. The key step of this mechanism is the electrophilic substitution reaction of the $H^+$ on the hydroxyl group with t-$C_4H_9^+$.[21] Besides the main reaction of 5-HMF etherification with IB to generate tBMF, dimerisation of 5-HMF and oligomerisation of IB also occur under the reaction conditions to form the symmetrical ether OBMF and DiB (a mixture of 2,4,4-trimethyl-1-pentene and 2,4,4-trimethyl-2-pentene), respectively. An significant amount of OBMF is formed from the using of certain homogeneous or solid acids at temperatures around 100–130 ℃.[19,22,23] In the present reactions, the reaction temperature, only 60 ℃, was very low; thus, 5-HMF dimerisation to OBMF is not a dominant reaction. DiB formation results in undesirable consumption of IB, and the compound is generally problematic when formulated with fuels.[24,25] As oligomerisation of IB is irreversible,[26] DiB formation must be minimised. Humins, which are the primary by-products of most reactions containing 5-HMF,[7,8] appeared in the liquid-acid catalysed reaction of 5-HMF etherification with IB, as evidenced by the darkening of colour of mixtures representing entries 7 and 8 reactions after conversion over *p*-TSA and $H_2SO_4$ catalysts, respectively. The mechanism of

Catalysis Science & Technology Accepted Manuscript

humin formation in this reaction is not fully understood, but humins have been proposed to form from oligomerisation of 5-HMF with other reactants and/or intermediates.[27,28] Formation of 5-HMF hydrolysates and *tert*-butanol may also occur in acid reactions because water is formed through dimerisation of 5-HMF, but these by-products are obtained in very small amounts. Scheme 2 summarises the main reaction pathways of the catalytic etherification of 5-HMF with IB.

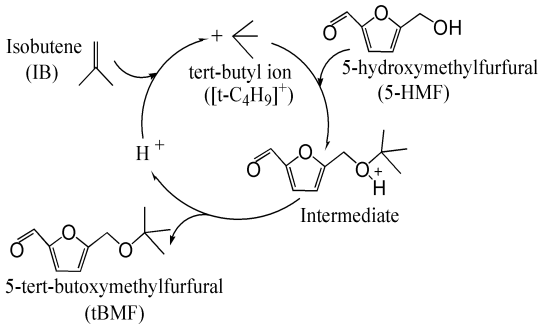


**Scheme 1.** Proposed reaction mechanism for etherification of 5-HMF with isobutene.

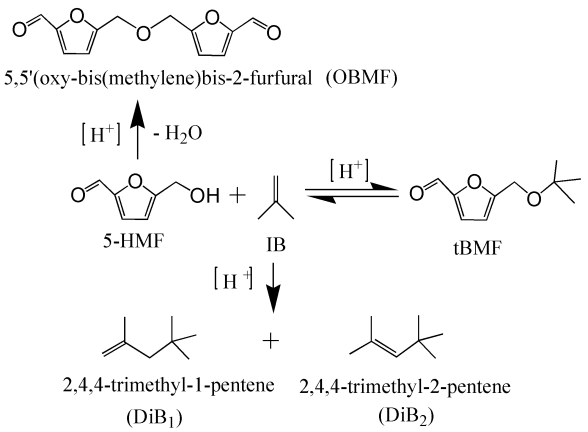


**Scheme 2.** Main reaction pathways of etherification of 5-HMF with isobutene in the presence of acid catalysts.

Catalytic performance strongly depended on the catalysts used. As shown in Table 2, entries 1–3, amongst the three HY zeolites, the sample with a $SiO_2/Al_2O_3$ ratio of 12 (HY-12) exhibited an excellent tBMF selectivity of 94 mol% and 59 mol% 5-HMF conversion. HY-80 also showed good selectivity toward tBMF, but the 5-HMF conversion achieved by this catalyst was 14 mol% lower than that achieved by HY-12. HY-5 demonstrated very low conversions; this result is quite different from those obtained for the aforementioned HY zeolites with higher $SiO_2/Al_2O_3$ ratios. HBeta showed moderate catalytic activity (5-HMF conversion, 24 mol%) and its tBMF selectivity was inferior to those over HY-12 and HY-80. 5-HMF conversions on HZSM-5-80 and HFER-55 were only 5 mol% and 2 mol%, respectively. Dimerisation of 5-HMF to form OBMF over these zeolites was trivial (no more than 2 mol%). Formation of OBMF involves the removal of one water molecule, which requires a high reaction temperature to provide adequate activation energy. Therefore, it was drastically suppressed at temperature as low as 60 ℃ with moderate acid sites on the zeolites. Another typical characteristic of the reactions over the zeolites is that oligomerisation of IB was minimal. Except for HBeta, which generated 3 wt% DiB, all other zeolites formed no more than 1 wt% DiB. For the reactions of 5-HMF etherification with IB, the mole ratio of IB:5-HMF was 4:1 or more, and IB was overloaded. Thus, the conversion of isobutene was low. The converted IB was consumed by tBMF and DiB as well as coke formations. Given the entry 2 reaction in Table 2 for example, only 15% IB was converted, and 96% converted IB was consumed by tBMF formation.

*p*-TSA and $H_2SO_4$ showed the catalytic activity necessary to convert 5-HMF but also generated undesired by-products. When working with *p*-TSA, about 43 mol% 5-HMF was converted with only 10 mol% selectivity towards tBMF. *p*-TSA has been used as a catalyst for the synthesis of OBMF.[22,29] In the present reaction, *p*-TSA also showed some catalytic activity towards OBMF formation since 23 mol% OBMF was generated over it. A relatively high conversion of 62 mol% was obtained over the $H_2SO_4$ catalyst after 3 h of reaction at 60 ℃, but its selectivity towards tBMF was only 27 mol%. Thus, homogeneous catalysts with high acidity are not suitable for 5-HMF conversion because they promote serious side reactions.

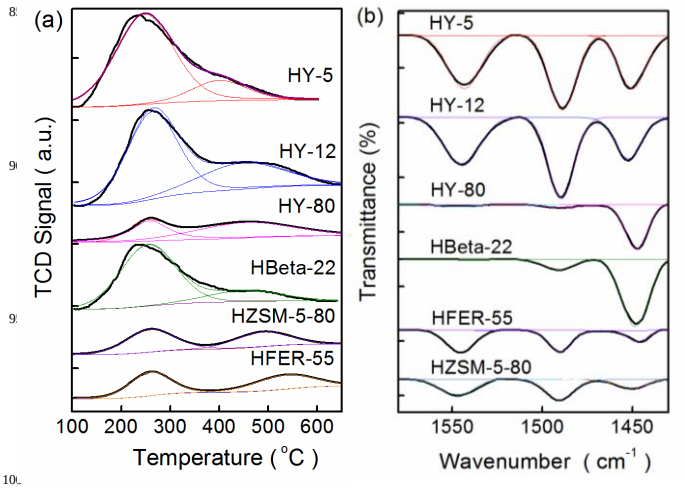


**Fig. 1.** $NH_3$-TPD profiles (a) and Pyridine-FT-IR spectra (b) of zeolites. Gaussian line shapes are deconvoluted into individual peaks using XPSPEAK 41.

**Table 3.** Type and amount of surface acid sites and Lewis/Brønsted (L/B) acidity ratios of the zeolite catalysts

| Entry | Catalyst | Total acid amount [a] (mmol g$^{-1}$) | Acid strength distributions [a] (mmol g$^{-1}$) | | Acid site distributions [b] (mmol g$^{-1}$) | | |
|---|---|---|---|---|---|---|---|
| | | | Weak | Strong | Lewis | Brønsted | L / B |
| 1 | HY-5 | 1.714 | 1.198 | 0.515 | 0.779 | 0.935 | 0.83 |
| 2 | HY-12 | 1.712 | 1.156 | 0.556 | 0.687 | 1.025 | 0.67 |
| 3 | HY-80 | 0.630 | 0.204 | 0.426 | 0.598 | 0.032 | 18.49 |
| 4 | HBeta-22 | 1.093 | 0.854 | 0.239 | 1.083 | 0.010 | 111.75 |
| 5 | HZSM-5-80 | 0.515 | 0.297 | 0.218 | 0.141 | 0.374 | 0.38 |
| 6 | HFER-55 | 0.497 | 0.266 | 0.231 | 0.170 | 0.327 | 0.52 |

[a]Determined by $NH_3$-TP D profile. [b]From $NH_3$-TPD and Py-FT-IR spectra.

Catalysis Science & Technology Accepted Manuscript


This journal is © The Royal Society of Chemistry [year]

Different acid properties (acid amount and acid strength), pore dimensions and topologies exert strong influences on the catalytic performance of zeolites. HY is a faujasite zeolite that has three-dimensional channels with super cages. The maximum diameter of a super cage of Y faujasite is about 12 Å, and all super cages are interconnected by 12-membered ring channels that possess comparable channel diameters of about 7.4 × 7.4 Å. The large channels enable the reactants and products to diffuse into or out of the super cages. Moreover, the super cages in Y faujasite zeolites provide sufficient space for configuring the transition-state structure of the intermediate and changing the position of tBMF towards the channel windows. Therefore, HY zeolites with large channels and super cages facilitate diffusion of the reactants and products and configuration of transition state. Since the three HY zeolites (Table 1, entries 1–3) have the same crystalline structures, differences in their catalytic performances may be attributed to their acid and adsorption properties. Fig. 1 shows the $NH_3$-TPD profiles and pyridine-FT-IR spectra of the zeolites. The type and amount of acid sites of the zeolites are quantified by $NH_3$-TPD and pyridine-FT-IR, as listed in Table 3. As shown in the $NH_3$-TPD profiles in Fig. 1(a), the large desorption peak at around 250 ℃ and the small desorption peak around 400 ℃ in the HY-5 curve manifests that this zeolite has sufficient weak acid sites and a few moderately strong acid sites. Weak acid sites (the desorption peak at around 250 ℃) on HY-12 are slightly fewer than those on HY-5, but the strong acid sites of HY-12 (the desorption peak at around 450 ℃) are more in number and stronger in acidity than those on HY-5. Increasing the framework $SiO_2/Al_2O_3$ ratio to 80 (HY-80) dramatically reduces the numbers of weak and strong acid sites. The effect of acidity was confirmed by correlating the reaction results in Table 2 with the acid properties in Fig. 1(a). HY-80, which presents a few strong-acid sites yielded more tBMF than HY-5, which presents a large number of weak-acid sites. This result reveals that the relatively stronger acidity of a zeolite is a prerequisite to generate efficient catalytic activity during reaction at a low temperature of 60 ℃.

Increasing the $SiO_2/Al_2O_3$ ratio of zeolite not only decreases the number of acid sites and increases its acid strength but also increases its surface hydrophobicity and decreases its polarity. Water is often used as a molecule probe to assess the zeolites' adsorption properties, *i.e.* hydrophilicity and hydrophobicity. Numerous studies have shown that water adsorption decreases when the framework Si/Al ratio of the zeolites increases, indicating that samples with lower framework-aluminium content are more hydrophobic.[30-32] tBMF production involves two compounds with different polarities (5-HMF is more polar than IB). Thus, a catalyst with optimal hydrophobicity and polarity can absorb the reactants 5-HMF and IB simultaneously, thereby promoting the conversion reaction towards more tBMF. The strong hydrophilic character of HY-5 favours extensive adsorption of reactants and products and blocks pores and acid sites, which, in combination with insufficient strong-acid sites, results in a less active catalysis. The catalytic activity of the more-hydrophobic zeolite HY-80 was controlled by its small number of acid sites, which is attributed to the very high $SiO_2/Al_2O_3$ ratio of this catalyst.

As shown in Fig. 1 and Table 3, HY-12 demonstrates a Lewis/Brønsted acid-site distribution similar to that of HY-5. However, HY-12 shows much higher catalytic activity in the etherification of 5-HMF with IB than that shown by HY-5 because the acid strength and surface prosperity of the zeolites play critical roles to determine the catalytic performance, as discussed above. The Brønsted acid sites are generally believed to catalyse the etherification reactions.[33,34] In the present reaction, the Lewis acid sites can also catalyse the reaction because HY-80 mainly contains Lewis acid (Table 3) and achieves an decent catalytic activity. As such, both Brønsted and Lewis acid sites catalyse the etherification of 5-HMF with IB. HY-12 exhibits considerable amount of both acids sites, which in combination with the sufficient acid strength, suitable adsorption properties and wide pore on structure can ensure high catalytic activity.

HBeta-22 shows lower activity in etherification whereas higher activity in DiB formation than HY-12 (Table 2). HBeta has 12-membered rings and tridirectional channels with small channel interactions (about 9 Å). Highly hydrophobic HBeta zeolites are excellent acid catalysts to perform selective etherification of 5-HMF with fatty alcohols (containing between C8–C18 carbon atoms).[35] Unlike fatty alkyls that have linear structures without branch chains, tBMF possesses a ternary branch structure; thus, etherification of 5-HMF with IB requires greater space to develop the transition-state configuration and to facilitate diffusion in the channels. In contrast to the super cages of HY, HBeta has no large cavities. As such, geometrical constraints within the pores of HBeta may be reasonably considered to result in low activity and selectivity toward the desired tBMF product. However, oligomerisation of IB on HBeta-22 is much higher than that on HY-12. In the reaction systems containing only IB (the reactions were held under the same reaction condition listed in the footnote of Table 2 but without 5-HMF participation), the DiB contents catalysed by HY-12 and HBeta-22 were 3 wt% and 49 wt%, respectively. HBeta-22 also catalysed the trimerisation of IB. Ji woong et al [36,37] investigated the oligomerisation of IB over several zeolite catalysts and found that the remarkable performance of the zeolites was presumably associated with the high Lewis site-to-Brønsted site ratio (L/B). Hence, the high activity of HBeta-22 in IB oligomerisation may be related to the high concentration of Lewis acid sites in HBeta-22, as revealed by the FT-IR study in combination with the $NH_3$-TPD results. The total acid amount of HBeta-22 is lower than that of HY-12 (Table 3). Moreover, tBMF exhibits a larger molecular size and poorer structural symmetry than those of DiB. Thus, the lower activity of HBeta-22 with respect to the HY-2 zeolite in tBMF formation can be attributed to the lower concentration of total acid sites and the diffusional constraints of HBeta-22.

HZSM-5 and HFER feature 10-membered ring channels, and their low catalytic activity for etherification of 5-HMF with IB is attributed to strong steric and diffusional constraints in these channels. The limited reactions of HZSM-5 and HFER occurred mainly on the external surface of the crystallites. Therefore, the desired activity and selectivity of a catalyst involves not only optimisation of the number and strength of its active sites and adsorption properties but also improving its internal pore space.

### 3.2. Influence of solvents

The present work was undertaken to study solvent effects using various aprotic organic solvents, including low-polarity (cyclohexane and toluene), moderate-polarity (dioxane, THF,

Catalysis Science & Technology Accepted Manuscript

glycol dimethyl ether and dichloromethane) and high-polarity (acetone, dimethyl sulphoxide and acetonitrile) solvents; the most polar solvent, water, was also evaluated for etherification of 5-HMF with IB over HY-12 zeolite at 60 ℃ (Table 4). Solvent polarities were quantified in terms of normalised molar electronic transition energies ( $E_T^N$ ) from UV/Vis/near-IR spectroscopic Measurements.[38] A smaller $E_T^N$ value means lower polarity of the solvent. Hence, the $E_T^N$ scale in Table 4 ranges from 0.006 for the least polar solvent, cyclohexane, to 1.000 for the most polar solvent, water.

**Table 4.** Effect of solvent on etherification of 5-HMF with IB.[a]

| Entry | Solvent | $E_T^N$ | Conversion (mol%) 5-HMF | Selectivity (mol%) tBMF | Yield (mol%) tBMF | Yield (mol%) OBMF | DiB (wt%) |
|---|---|---|---|---|---|---|---|
| 1 | cyclohexane | 0.006 | 12 | 43 | 5 | 2 | 1 |
| 2 | toluene | 0.099 | 21 | 63 | 13 | 4 | <1 |
| 3 | dioxane | 0.164 | 26 | 67 | 17 | <1 | 1 |
| 4 | THF | 0.207 | 39 | 93 | 36 | 1 | <1 |
| 5 | glycol dimethyl ether | 0.231 | 59 | 94 | 55 | <1 | <1 |
| 6 | dichloromethane | 0.309 | 32 | 70 | 22 | 2 | 3 |
| 7 | acetone | 0.355 | 13 | 46 | 6 | 1 | <1 |
| 8 | dimethyl sulphoxide | 0.444 | 5 | - | - | - | - |
| 9 | acetonitrile | 0.460 | 6 | - | - | - | - |
| 10 | water | 1.000 | 0 | - | - | - | - |

[a] Reaction conditions: $R_{IB/5\text{-}HMF}$, 4 mol/mol; catalyst loading, 30 wt%; 100 mg of 5-HMF in 1 mL of solvent; 60 ℃; 3 h.

As $E_T^N$ increased in the range of 0.006–1.000, 5-HMF conversion showed a volcano-like trend. Only 12 mol% 5-HMF conversion was observed in the apolar cyclohexane solvent. While a high conversion of 59 mol% with an excellent tBMF selectivity of 94% was achieved in glycol dimethyl ether solvent with 0.231 $E_T^N$ value. When the reactions were tested in dimethyl sulphoxide and acetonitrile aprotic solvents, conversion rapidly decreased because of the strong polarities of the solvents. Water in the reaction system inhibited tBMF formation mainly because water can hydrolyse the tBMF product, which is the reason that conversion of 5-HMF is difficult to get a very high value in etherification of 5-HMF with *tert*-butanol due to water formation.[17,18] Solvent effects were less significant for by-product formation than for tBMF yield. OBMF yields and DiB contents observed in a variety of solvents were within 4 mol% and 3 wt%, respectively. Solvent properties include many aspects that may exert specific effects on the reaction systems. For instance, hydrogen bonding, preferential solvation, acid–base chemistry and/or charge–transfer interactions may exert specific effects.[39] Solvent polarities plays substantial roles on the local environment in a reaction system, partly observed from interactions between the reactants/products and solvent molecules or between solvent molecules and the catalyst surface. Cyclohexane and toluene as non-polar or low-polarity solvents prefer to dissolve lipophilic IB, but these solvents exhibit insufficient ability to remove the polar product molecule from the catalyst surface. Solvents with strong polarity are prone to adsorption on the catalysts and hinder the adsorption of reactants, as indicated by the negative effects of strongly polar solvents such as dimethyl sulphoxide and acetonitrile described above. Glycol dimethyl ether and THF with suitable polarities present balanced hydrophilic/hydrophobic properties that benefit adsorption of the reactants and desorption of the product. Thus, optimal catalyst activity was observed not in lowly or strongly polar solvents but in moderately polar solvents. All these aspects considered, glycol dimethyl ether is the most suitable solvent for this reaction. The relatively low boiling point of glycol dimethyl ether (85 ℃) further allows significant energy savings during recovery of tBMF by distillation.

Results in Table 4 show that the lower conversions tend to correspond to the lower selectivities. Although the etherification of 5-HMF with IB was restrained significantly in lowly or strongly polar solvents, the reactions towards by-products such as coke and/or OBMF remained active. Reactions in all the organic solvents from low-polarity cyclohexane to high-polarity acetonitrile more or less formed coke on the catalysts, which has been confirmed by the dark colours of the spent catalysts and their TG results. For instance, following the reaction in cyclohexane solvent, the catalyst became brown in colour. The TGA result (not shown here) indicated that the coke amount was approximately 17 wt% with respect to the fresh catalyst mass. This finding demonstrated that approximately 5 mg of coke was formed in the reaction system containing 100 mg of 5-HMF. Formation of coke consumed a few 5-HMF. The incapability of the cyclohexane solvent in driving tBMF off the catalyst aggravates coke formation. When only 12% of 5-HMF is converted, the coke and OBMF (2 mol% in yield) as well as other by-products account for obvious shares in the final product. As a result, the tBMF selectivity was only 43 mol% when reacted in cyclohexane.

### 3.3. Influences of reaction conditions

Fig. 2 shows that increasing the reaction temperature exerts a significant impact on the reaction performance. tBMF selectivity remains nearly constant and is maintained at 90% and higher from 40 ℃ to 70 ℃; at temperatures higher than 70 ℃, a gradual decrease in selectivity is observed. High selectivity towards tBMF indicates that the catalyst favours formation of tBMF. As temperature increased in the range of 40–100 ℃, conversion of 5-HMF exhibited a volcano-like trend with a maximal value (59 mol%) achieved at 60 ℃. Because 5-HMF etherification with IB is a moderately exothermic reaction, a relatively higher reaction temperature is necessary to provide adequate activation energy. However, excessive heat favours the reverse reaction, which leads to increase in dealkylation of tBMF and lower 5-HMF

Catalysis Science & Technology Accepted Manuscript


This journal is © The Royal Society of Chemistry [year]

conversion. Too-high temperatures also accelerate side reactions. As shown in Fig. 2, less than 1.0 wt% DiB is observed at 40–90 ℃; when the temperature rises to 100 ℃, over 1.0 wt% DiB formation is observed. OBMF yield also increases with the temperature. Moreover, too high temperature aggravated other side reactions and accelerated the deactivation of the catalyst, as indicated by the dark coloured mixture obtained after reaction at higher temperatures. Considering these findings, 60 ℃ can be regarded as the optimal temperature for etherification over the catalyst.

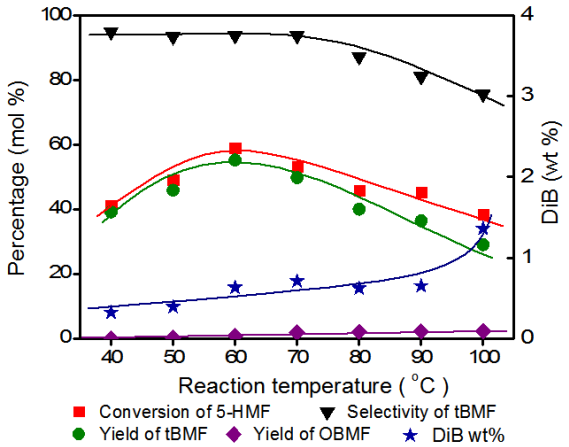


**Fig. 2.** Influence of reaction temperature on 5-HMF etherification with IB (Reaction conditions: $R_{IB/5\text{-}HMF}$, 4 mol/mol; catalyst loading, 30 wt%; 3 h).

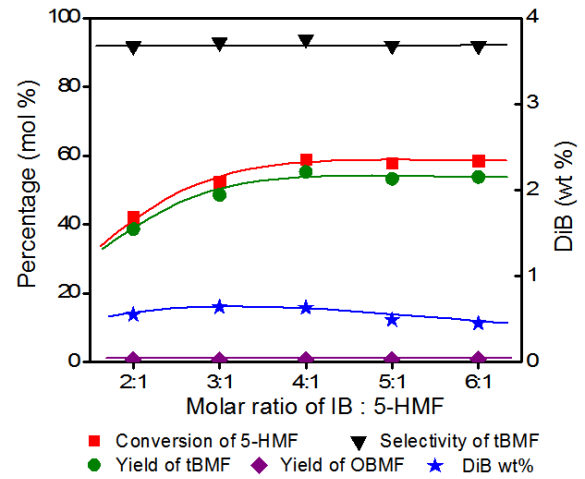


**Fig. 3** Etherification of 5-HMF with isobutene at different IB:5-HMF mole ratio (Reaction conditions: catalyst loading, 30 wt%; 60 °C; 3 h).

Fig. 3 shows the effect of IB loading amount on the reaction performance. With the increase in IB:5-HMF mole ratio in the range of 2:1 to 4:1, a gradual increase in 5-HMF conversion is observed; at IB:5-HMF mole ratio higher than 4:1, 5-HMF conversion remains nearly constant. The tBMF selectivity and OBMF yield are nearly independent of the mole ratio of IB:5-HMF. DiB wt% changes little and even decreases slightly with increasing IB:5-HMF ratio. But the absolute amount of DiB is triple when IB:5-HMF ratio increases from 2:1 to 6:1. Sufficient IB in the reaction system benefits the forward reaction towards tBMF formation, but too high IB concentration is prone to self condensation, forming DiB. Weighed the pros and cons, IB:5-HMF mole ratio of 4:1 is desirable.

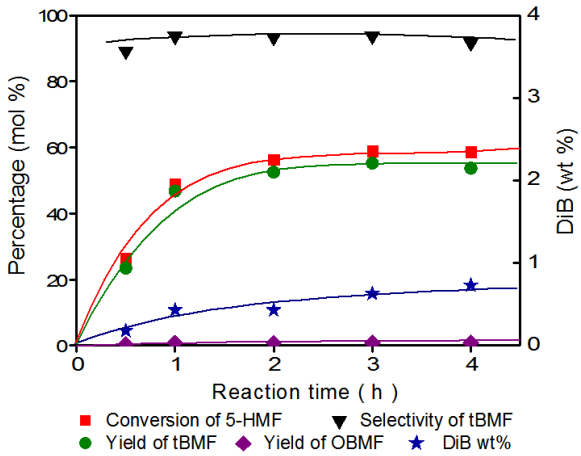


**Fig. 4.** Etherification of 5-HMF with isobutene at different reaction time (Reaction conditions: $R_{IB/5\text{-}HMF}$, 4 mol/mol; catalyst loading, 30 wt%; 60 °C).

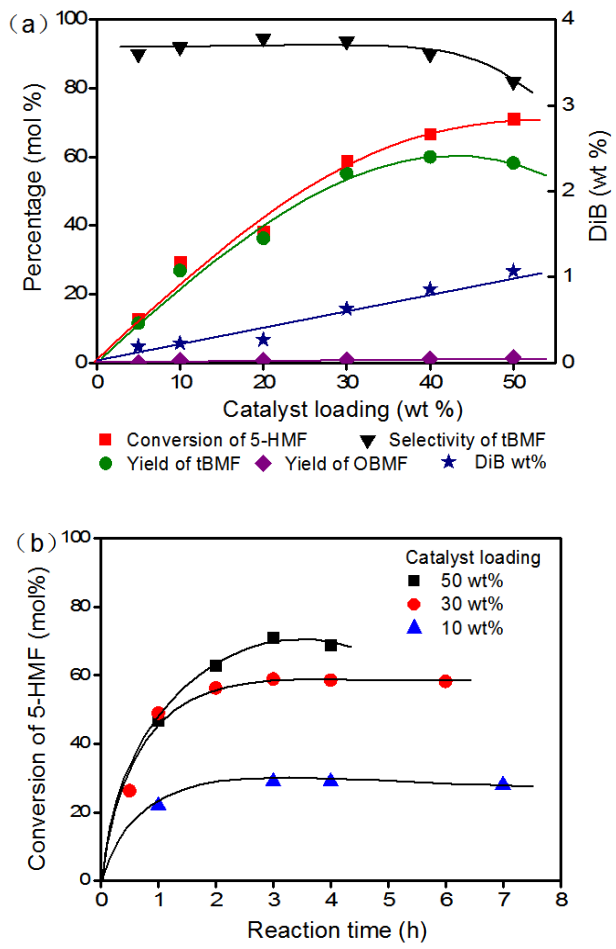


**Fig. 5.** Influence of catalyst loading on 5-HMF etherification with isobutene: (a) at the same reaction time of 3 h; (b) at different reaction time (Reaction conditions: $R_{IB/5\text{-}HMF}$, 4 mol/mol; 60 °C).

Catalysis Science & Technology Accepted Manuscript

The reaction results as functions of the reaction time are depicted in Fig. 4. Conversion of 5-HMF increases with reaction time and then reaches a plateau. Notably, the selectivity to tBMF is more than 90 mol% during the testing time. DiB and OBMF yields gradually increase with prolonged reaction time, indicating that formations of the by-products are an irreversible reaction, but these side reactions are not serious since the upward trends are not steep. Subsequently, the effects of the catalyst loading on the performance of HY-12 are investigated (Fig. 5). Yield of tBMF increases from 12 mol% to 60 mol% when the catalyst loading is increased from 5wt% to 40 wt% (Fig. 5a). However, further increase of the catalyst loading results in a drop in tBMF yield, since side reactions such as coke formation are promoted by long contact time with the catalyst. Similar to high temperature and long reaction time, high catalyst loading also promotes IB oligomerisation and 5-HMF dimerisation. DiB content and OBMF yield exceed 1 wt% and 1 mol%, respectively, when the catalyst loading increases to 50 wt%. As shown in Fig. 4, although the initial reaction is fast, an equilibrium seems to be reached at 3h since the conversion of 5-HMF remained at about 59 mol% to the end of the test. However, the reaction with a higher catalyst loading shows a continuous increase of 5-HMF conversion that surpasses the one with a lower loading (Fig. 5b). Therefore, the reaction in Fig. 4 is not limited by equilibrium restraint. It is possible to achieve a very high conversion as long as the reaction system keeps its catalytic activity. The conversion plateau observed in Fig. 4 after 3 h is due to catalyst deactivation, as shown below.

### 3.4. Recyclability of catalyst

**Table 5.** Studies of catalyst reuse of HY-12.

| Entry | Catalyst | $S_{BET}$ ($m^2$/g) | $V_{Pore}$ ($m^2$/g) | Conver. (mol%) 5-HMF | Yield (mol%) tBMF | Yield (mol%) OBMF | DiB (wt%) |
|---|---|---|---|---|---|---|---|
| 1 | Fresh HY-12 | 740 | 0.46 | 59 | 55 | <1 | <1 |
| 2 | Spent HY-12 | 505 | 0.34 | 6 | 4 | <1 | <1 |
| 3 | Calcined HY-12 | 735 | 0.46 | 58 | 56 | <1 | <1 |

Reaction conditions: $R_{IB/5\text{-}HMF}$, 4 mol/mol; catalyst loading, 30 wt%; 100 mg of 5-HMF in 1 mL of glycol dimethyl ether; 60 °C; 3 h.

The reusability of HY-12 for etherification of 5-HMF with IB in the glycol dimethyl ether solvent system was investigated. The spent HY-12 obtained after successive washing with solvents and drying showed very poor activity (Table 5, entry 2). However, after calcination of the spent HY-12 in air, 5-HMF conversion and tBMF selectivity over the calcined HY-12 (Table 5, entry 3) were comparable with the corresponding values obtained from the fresh catalyst (Table 5, entry 1). This result reveals that catalytic activity can be fully recovered by calcination of HY-12 in air. SEM images shown in Fig. 6 demonstrate that the fresh, spent and calcined HY-12 catalysts present very similar morphologies, which means deactivation does not occur through build-up of coke on the external surface of the catalyst particles. The signal strengths in the XRD patterns in Fig. 6 further indicate that spent and calcined HY-12 retain the typical texture of the Y faujasite framework, as evidenced by signals at characteristic 2 theta values of 6.3 °, 10.3 °, 12.1 °, 16.0 °, 19.0 °, 20.8 °, 24.1 ° and 27.6 °; loss of crystallinity of the spent and calcined zeolites, if any, was minimal. Thus, the relatively low activity of spent HY-12 does not result from any destruction of the zeolite structure. The plots of the pore volume vs. pore diameter (dV/dD) curves of the fresh HY-12 and spent HY-12 (not shown here) manifest that the dV/dD peak of the spent HY-12 in the micropore section is much smaller with slightly less pore diameter than that of the fresh HY-12, indicating the narrowing of the pore openings as a result of coke formation in the zeolite framework. Thus, clockage of catalyst pores by bulkier molecules formed during the course of the reaction may explain the catalyst deactivation observed. The diminished specific surface area and pore volume of the spent catalyst further confirms this conclusion as compared to the fresh one (in Table 5).

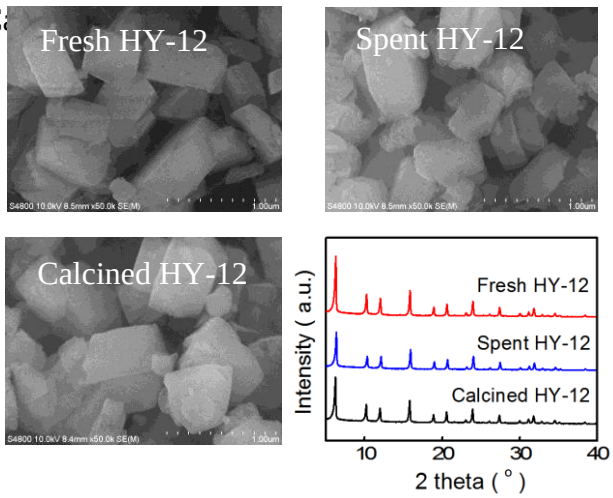


**Fig. 6.** SEM images and XRD patterns of the fresh, spent and calcined HY-12.

**Table 6.** Stepwise-feeding conversions of 5-HMF and/or IB over HY-12.

| Entry | Reactant | Reactant conditions | Conver. (mol%) 5-HMF | Yield (mol%) tBMF | Yield (mol%) OBMF | DiB (wt%) |
|---|---|---|---|---|---|---|
| 1 | 5-HMF | 100 mg of 5-HMF in 1 mL of glycol dimethyl ether | 4 | | 1 | |
| 2 | 5-HMF+IB | After entry 1 reaction, 178 mg of IB was loaded | 57 | 52 | 1 | <1 |
| 3 | IB | 178 mg of IB in 1 mL of glycol dimethyl ether | | | | 3 |
| 4 | IB+5-HMF | After entry 3 reaction, IB was discharged; 100 mg of 5-HMF and 178 mg of IB were loaded | 58 | 56 | <1 | 4 |

Supplementary reaction conditions: catalyst loading, 30 wt%; 60 °C; 3 h.

Catalysis Science & Technology Accepted Manuscript


This journal is © The Royal Society of Chemistry [year]

Catalysis Science & Technology

Cite this: DOI: 10.1039/c0xx00000x

www.rsc.org/xxxxxx

PAPER

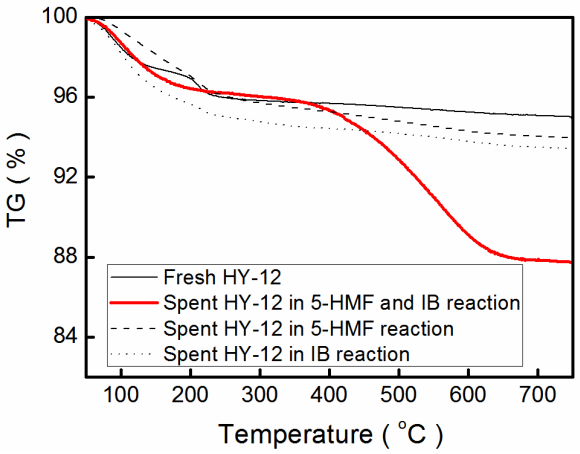


**Fig. 7.** TGA profiles of fresh HY-12, spent HY-12 during etherification of 5-HMF with IB, spent HY-12 during the 5-HMF reaction and spent HY-12 during the IB reaction.

To understand the deactivation pathway of HY-12, a series of control tests was performed by employing stepwise-feeding reactions. As shown in Table 6, entry 1, when the reaction is performed over HY-12 without IB participation, 5-HMF is converted by 4 % (the actual conversion is below 4 mol% because of absorption by the catalyst and share of impurities in feed) and 1 mol% of OBMF is obtained. This result demonstrates that dimerisation of 5-HMF on HY-12 under mild reaction conditions does not occur extensively. The HY-12 catalyst obtained after entry 1 further catalysed etherification of the remained 5-HMF with IB subsequently loaded to achieve 57 mol% 5-HMF conversion and 52 mol% tBMF yield (Table 6, entry 2). This result demonstrates that side reactions of 5-HMF dimerisation are not the primary factor causing coke deposition in the pores of the catalyst. Oligomerisation of IB as another typical side reaction was investigated on the basis of the reactions listed in entries 3 and 4 in Table 6. In the reaction system containing only IB, 3 wt% DiB was formed after reacting over HY-12 for 3 h at 60 ℃ (Table 6, entry 3). In the case of reaction 4, a conversion of 58% and high tBMF yield of 56 mol% were achieved over the HY-12 catalyst after use in entry 3. Similar to dimerisation of 5-HMF, oligomerisation of IB is not responsible for the extensive coke deposition observed in the pores of the catalyst.

TGA profiles of fresh and spent HY-12 after catalysing particular reactions are shown in Fig. 7. The TGA curve of fresh HY-12 shows a weight loss between 50 and 250 ℃, which is attributed to evaporation of residual moisture. The spent HY-12 catalyst obtained after etherification of 5-HMF with IB shows a sharp weight loss (about 8 wt% relative to the catalyst mass) beginning from 400 ℃ and ending at 600 ℃; a weight loss peak attributed to moisture evaporation is also observed at around 150 ℃. Weight loss at higher temperatures (around 500 ℃) is attributed to the combustion of coke deposited on the catalyst.[40] The TGA profiles of spent HY-12 catalyst collected from 5-HMF dimerisation and IB oligomerisation are very similar to that of the fresh catalyst. These TGA results indicate that coke is predominantly deposited on the catalyst during etherification of 5-HMF with IB. Such conclusions are in good agreement with reaction results showing that rapid loss of activity of the HY-12 catalyst does not occur in reaction systems containing either 5-HMF or IB only but occurs in the system containing both 5-HMF and IB. tBMF is not likely to be the main substrate for forming the deposited coke because it can diffuse in the HY channels. Thus, accumulation and progression of coke deposition must be attributed to geometrical constraints conferred by bulkier products formed through consecutive reactions such as IB oligomerisation and further etherification of 5-HMF with DiB or humin formation

## 4. Conclusions

In summary, the biodiesel additive, tBMF, is synthesised through etherification of 5-HMF with IB on a series of acid zeolites and two types of liquid acids, *i.e.*, *p*-TSA and $H_2SO_4$, at moderate conditions. Different acid properties (*i.e.*, acid amount and acid strength), pore dimensions and topologies exert strong influences on catalytic performances of the zeolites. Amongst the zeolites studied, HY zeolite with special features showed desirable catalytic activity and high selectivity towards tBMF; these features are attributed to the adequacy of active sites and adsorption properties as well as the internal pore space of the catalyst. 5-HMF conversions in solvents with either very weak or very strong polarity were obviously lower than that in solvents with moderate polarity. Glycol dimethyl ether with such a suitable polarity exhibited excellent solvent effect in the reaction. The HY zeolite with a $SiO_2/Al_2O_3$ mole ratio of 12 (HY-12) in combination with glycol dimethyl ether solvent exhibited an excellent selectivity of 94 mol% towards tBMF and 59 mol% 5-HMF conversion after 3 h of reaction at 60 ℃. Side reactions of 5-HMF dimerisation to OBMF and IB oligomerisation to DiB over zeolites were minimal under mild reaction conditions. Catalytic reactions on *p*-TSA and $H_2SO_4$ were not desirable because the strong acidities of these homogeneous catalysts led to serious side reactions. Deactivation of HY-12 was caused by coke deposition in the pores of the catalyst; the activity of the deactivated catalyst was fully recovered with calcination in air.

## Acknowledgements

This work was supported by the National Natural Science Foundation of China (Grant Nos. 21203015 and 21173027) and the Chinese Central Government "Thousand Talent Program" Funds. The Department of Education of Liaoning Province

Catalysis Science & Technology Accepted Manuscript

(China) and the State Key Laboratory of Fine Chemicals at Dalian University of Technology (Grant No. KF1109) also provided financial support.

## References


1 M. Crocker, Thermochemical conversion of biomass to liquid fuels and chemicals, Royal Science and Chemistry, 1st edition, 2010.

2 A. Sarin, Biodiesel: Production and properties, Chapter 5, Low-temperature flow properties of biodiesel, Royal Society of Chemistry, 1st edition, 2012, 80-106.

3 L. Ha, J. Mao, J. Zhou, Z. C. Zhang and S. Zhang, *Appl.Catal. A: Gen.*, 2009, **356(1)**, 52-56.

4 M. J. Climent, A. Corma and S. Iborra, *Green Chem.*, 2014, **16**, 516–547.

5 J. Zhou, Y. Wang, X. Guo, J. Mao and S. Zhang, *Green Chem.*, 2014, **16 (11)**, 4669-4679.

6 T. S. Viinikainen, R. S. Karinen, A. O. Krause, in: G. Centi, R. A. van Santen (Eds.), Production, Wiley-VCH Verlag GmbH and Co. KgaA, Weinheim, 2007.

7 R.J. van Putten, J. C. van der Waal, E. de Jong, C. B. Rasrendra, H. J. Heeres and J. G. de Vries, *Chem. Rev.*, 2013, **113**, 1499–1597.

8 H. Zhao, J. E. Holladay, H. Brown and Z. C. Zhang, *Science*, 2007, **316**,1596–1600.

9 G. J. M. Gruter and F. Dautzenberg, EP Pat., 2011/0082304, 2011.

10 E. R. Sacia, M. Balakrishnan and A. T. Bell, *J. Catal.*, 2014, **313**, 70–79.

11 P. Che, F. Lu, J. Zhang, Y. Huang, X. Nie, J. Gao and J. Xu, *Bioresource Technol.*, 2012, **119**, 433–436.

12 P. Lanzafame, D.M. Temi, S. Perathoner, G. Centi, A. Macario, A. Aloise and G. Giordano, *Catal. Today*, 2011, **175**, 435–441.

13 H. Noureddini, US Pat., 6015440, 2000.

14 M. Gupta, N. Kumar, *Renewable and Sustainable Energy Rev.*, 2012, **16**, 4551–4556.

15 R. Sarin, R. Kumar, B. Srivastav, S. K. Puri, D. K. Tuli, R. K. Malhotra and A. Kumar, *Bioresour. Technol.*, 2009, **100**, 3022-3028.

16 M. Rose, K.Thenert, R. Pfützenreuter and R. Palkovits, *Catal. Sci. Technol.*, 2013,3, 938-941.

17 G. J. M. Gruter, US Pat., 0,218,416 A1, 2010.

18 E. Salminen, N. Kumar, P. Virtanen, M. Tenho, P. Maki-Arvela and J. P. Mikkola, *Top Catal.*, 2013, **56**, 765–769.

19 Ch. Baerlocher, W. M. Meier, D. H. Olson, *Atlas of zeolits framework types*, Elsevier, 2001.

20 O. Casanova, S. Iborra, A. Corma, *J. Catal.*, 2010, **275**, 236–242.

21 J. Zhou, X. Liu, S. Zhang, J. Mao and X. Guo, *Catal. Today*, 2010, **149**, 232–237.

22 R.M. Musau and R.M. Munavu, *Biomass*, 1987, **13**, 67–74.

23 H. Wang, Y. Wang, T. Deng, C. Chen, Y. Zhu, X. Hou, *Catal. Commun.*, 2015, **59**, 127–130.

24 J. A. Melero, G. Vicente, G. Morales, M. Paniagua, J. M. Moreno, R. Roldán, A. Ezquerro and C. Pérez, *Appl. Catal. A: Gen.*, 2008, **346**, 44–51.

25 H. J. Lee, D. Seung, I. N. Filimonov and H. Kim, *Korean J. Chem. Eng.* , 2011, **28**, 756 –762.

26 K. Klepacova, D. Mr avec and M. Bajus, *Appl. Catal. A: Gen.*, 2005, **294**, 141–147.

27 Y. Román-Leshkov, J. N. Chheda and J. A. Dumesic, *Science*, 2006, **312**, 1933–1937.

28 H. Li, W. Xu, T. Huang, S. Jia, Z. Xu, P. Yan, X. Liu and Z. C. Zhang, *ACS Catal.*, 2014, **4 (12)**, 4446–4454.

29 D. Chundury and H.H. Szmant, *Ind. Eng. Chem. Prod. Res. Dev.*, 1981, **20**, 158–163.

30 D.H. Olson, W.O. Haag and W.S. Borghard, *Micropor.and Mesopor. Mat*,. 2000**, 35–36,** 435–446.

31 A. H. Yonli, I. Gener and S. Mignard, *Micropor. and Mesopor. Mat.*, 2009, **122**, 135–142.

32 M. J. Climent, A. Velty and A. Corma, *Green Chem.*, 2002, **4**, 565–569.

33 M. D. Gonzalez, P. Salagre, E. Taboada, J. Llorca, E. Molins and Y. Cesteros, *Appl. Catal., B*, 2013, **136–137**, 287–293.

34 J. Zhou, Y. Wang, X. Guo, J. Mao and S. Zhang, *Green Chem.*, 2014, **16 (11)**, 4669-4679.

35 K. S. Arias, M. J. Climent, A. Corma and S. Iborra, *ChemSusChem*, 2014, **7**, 210 – 220.

36 J. W. Yoon, J. S. Chang, H. D. Lee, T. J. Kim and S. H. Jhung, *J. of Catalysis*, 2007, **245**, 253–256.

37 J. W. Yoon, J. H. Lee, J. S. Chang, D. H. Choo, S. J. Lee and S. H. Jhung, *Catal. Commun.*, 2007, **8**, 967–970.

38 C. Reichardt, *Chem. Rev.*, 2002, **94(8)**, 2319-2358.

39 J. R. Lakowicz, Principles of fluorescence spectroscopy, chapter 6 solvent and environmental effects, Springer-Verlag, 3rd edition, 2006, 205-235.

40 K. Krishna, M. Makkee, *Appl. Catal. B: Environ.*, 2005, **59**, 35–44.


Catalysis Science & Technology Accepted Manuscript


This journal is © The Royal Society of Chemistry [year]